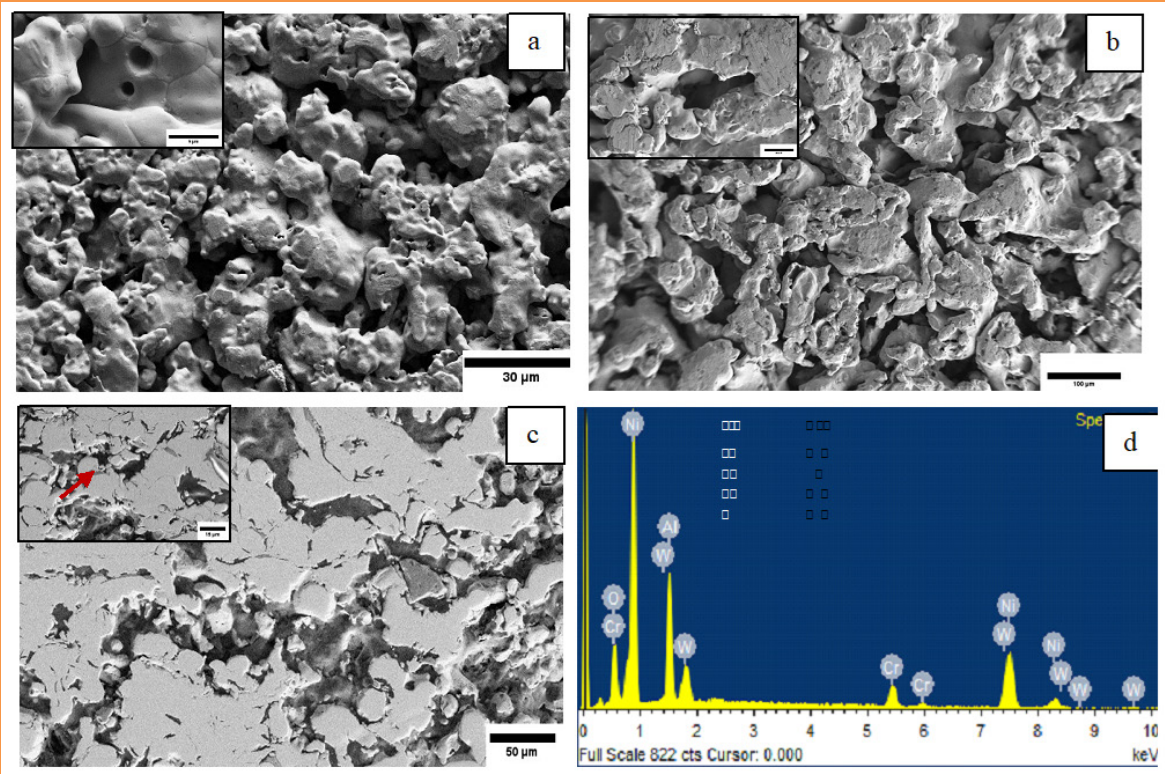


SPRAYTODAY®

An INSCIENCEIN publication | Affiliated to The Indian Thermal Spray Association®



Issue Highlights

- **Featured Article:** Non-destructive Evaluation of Porosity in Thermally Sprayed Coatings Using Permeability Measurement
- **Academia Research:** An Attempt to Understand Stainless 316 Powders for Cold-Spray Deposition
- **Industry Research:** Dense Sinkor® Coating for Sink Roll Application
- **2nd National Thermal Spray Conference & Expo 2025** and Pre-Conference course

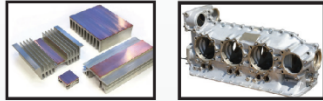
SPRAYCOLD

(COLD SPRAY SYSTEM)



MCS-23
with inbuilt heater

Hybrid Heat Sink Engine Crank Case



Prevent & Repair Damage.



MSC-500

(MEC cold spray system with trolley, powder feeder and PLC controlled panel.)

Application of Cold Spray

- ▲ Repair bearing seats.
- ▲ Repair forms & patterns for casting.
- ▲ Hermetically seal radiators and air conditioner.
- ▲ Add electrical conductive layers to materials.
- ▲ Additive manufacturing and many more.

Special Features:

- ▲ The detachable type control screen can be removed and positioned on another stand or exterior wall of the spray chamber if user wants to spray using robot/manipulator.
- ▲ Working Gas: Air or Nitrogen
- ▲ Single Phase Electrical Supply Requirement.

Maximum power consumption:- 3.3kW

Power supply:- Single Phase 220v, 50/60Hz

Powder consumption:- 10-60 gm/min
(compatible powder will be supplied by MEC)

Capacity of Powder Feeder:- 3350 CC (3.3 Liter)

Dimensions and Weight of the System:-
Approx. 600(W)x500(L)x1400(H)
Approx. 110 kg

MEC MX 1

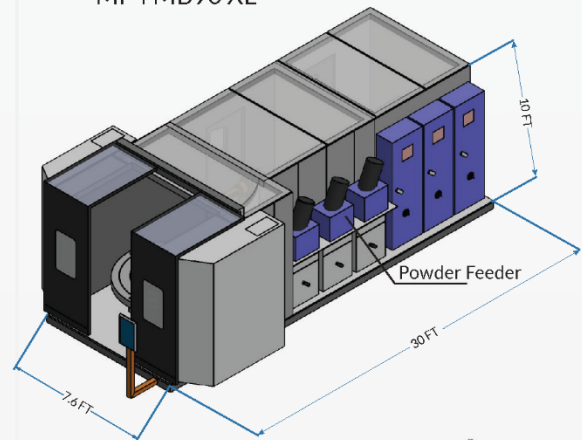
(INTEGRATED THERMAL SPRAY SYSTEM
for PLASMA /HVOF/HVOLF)



Cascaded Gun



MF4 MB90 XL



Standard Features:

- ▲ Standard and compact design
- ▲ User friendly interface to improve productivity
- ▲ Safety interlock to protect job by monitoring & controlling parameters
- ▲ Easy to transport and relocate to other facilities
- ▲ Data logging and report generation

Additional Features:

- ▲ Particle diagnostics, job temperature, process video on a single screen.
- ▲ Job cooling arrangement - air cooling by flow through the job utilizing rotary fluid adaptors.



METALLIZING EQUIPMENT CO. PVT. LTD.

ISO 9001:2015
ISO 17025:2017
AS 9100D, CE

Email:-marketing@mecpl.com / sales@mecpl.com Ph. : +91-291-2747601 Fax : 2746359

www.mecpl.com

SPRAYTODAY™

An INSCIENCEIN publication | Affiliated to the Indian Thermal Spray Association®

CHIEF EDITOR

Dr. Satish Tailor, MECPL Jodhpur, India.

INDIAN THERMAL SPRAY ASSOCIATION EXECUTIVE COMMITTEE & Editorial Board

Prof. Harpreet Singh, *President*
Prof. S Bakshi, *VP (Academia)*
Dr. RM Mohanty, *VP (Industry & Lab)*
Dr. Satish Tailor, *General Secretary*
Prof. Anup Kumar Keshri, *Joint Secretary*
Prof. Kamaraj M, *Senior Executive Member*
Prof. Jyotsna Dutta Majumdar, *Executive Member*
Dr. Sisir Mantry, *Executive Member*
Prof. Shashi Bhushan Arya, *Executive Member*

Mission: Our mission is to deliver the most recent thermal spray industry news and keep up to date to the thermal spray community by providing company, event, people, product, research, and membership news of interest to industrial leaders, engineers, researchers, scholars, policymakers, and the public thermal spray community.

SPRAYTODAY™ is a quarterly publication of the INSCIENCEIN Publishing, affiliated to the Indian Thermal Spray Association® [ITSA]. Published and distributed digitally INSCIENCEIN Publishing. Copyright© 2024 **The Indian Thermal Spray Association** is a standing committee of the "ITSA Association for Thermal Spray Technology and Research®", India.

ITSA and INSCIENCEIN Publishing are not responsible for the accuracy of information in the editorial, articles, and advertising sections of this publication. Readers should independently evaluate the accuracy of any statement in the editorial, articles, and advertising sections of this publication that are important to him/her and rely on his/her independent evaluation.

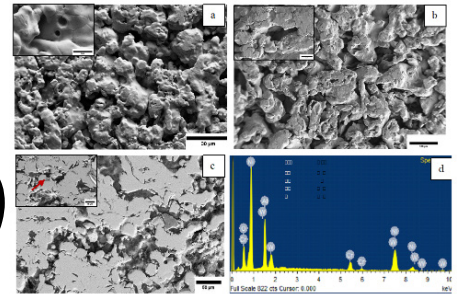
A subscription to **SPRAYTODAY™** is free for individuals interested in the thermal spray and coatings industry.

<http://www.inscience.in/spraytoday.html>

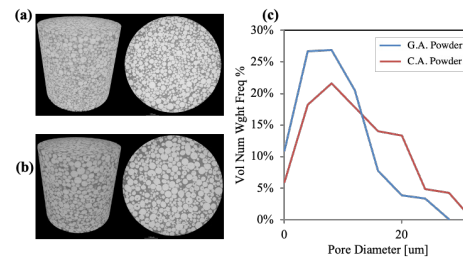
Write us spraytoday@inscience.in

Contents

9



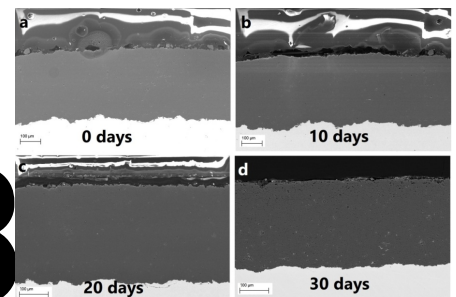
Featured Article: Non-destructive Evaluation of Porosity in Thermally Sprayed Coatings Using Permeability Measurement



14

Academic Research: An Attempt to Understand Stainless 316 Powders for Cold-Spray Deposition

18



Industry Research: Dense Sinkor® Coating for Sink Roll Application

SPRAYTODAY™

An INSCIENCEIN publication | Affiliated to the Indian Thermal Spray Association®

Indian Thermal Spray Asso. Membership 20

Official Journal Publication of the iTSA 20

ABOUT THE COVER

Representative SEM taken from (a-b) sintered porous discs with average pore sizes of 2 μm and 40 μm , (c) NiCrAlW coating along with its (d) EDS elemental spectrum

To contribute an article, advertisement, subscription request, back issue copies, and changes of address should be sent to:

spraytoday@inscience.in

METALLIZATION WIRES



World Leaders In:

- Zinc Wire/Rods
- Zn-Al alloy Wire
- Aluminium Wires
- Tin-Zinc Wires
- Tin Babbit Spray Wire
- Other Spray metallization Wires

KOTHARI METSOL PVT. LTD.

Formerv Khosla Engineering Pvt. Ltd.
An ISO 9001 : 2015 & 14001:2015 Certified Company

 Gat No. 130, Village Dhanore Off Alandi Markal Road, Tal - Khed, Dist- Pune 412105
 www.khoslaengineering.com

 sales@khoslaengineering.com

 +91 2135 6578403/412

Editor's Note



Dear Readers,

Welcome to the latest edition of **SPRAYTODAY** Magazine, your premier source for all things related to thermal spray technology. We are thrilled to bring you this special issue, which not only highlights the latest advancements and trends in thermal spray field but also looks forward to one of the most significant event on the thermal spray calendar: the **2nd Indian Thermal Spray Conference and Expo (NTSC2025)** <https://www.indtsa.org/ntsc-2025>. Scheduled to take place from February 21-22, 2025, at the esteemed CSIR-Institute of Minerals & Materials Technology (IMMT) in Bhubaneswar, this conference promises to be a hub of innovation and collaboration. The event will gather leading experts, researchers, and industry professionals from around the globe to discuss cutting-edge developments, share insights, and explore the future of thermal spray technology. With a robust lineup of keynote speeches, technical sessions, and an expansive expo showcasing the latest equipment and materials, this conference is set to elevate our understanding and application of thermal spray techniques.

In this issue, we are also delighted to feature a series of articles that delve into the recent trends shaping the thermal spray industry. Our contributors have explored a range of topics, from advancements in coating materials and application methods to the integration of artificial intelligence and automation in thermal spray processes. These articles provide a comprehensive overview of the current state of technology and offer a glimpse into the innovations that are driving the industry forward.

I am particularly pleased to be allowed to recommend to you the latest issue of the **SPRAYTODAY**. This issue includes invited innovative featured articles from industry and academia experts on “Non-destructive Evaluation of Porosity in Thermally Sprayed Coatings Using Permeability Measurement; An Attempt to Understand Stainless 316 Powders for Cold-Spray Deposition; Dense Sinkor® Coating for Sink Roll Application”, that illustrate current research trends in thermal spray development.

As we navigate the pages of this magazine, let's collectively embrace the spirit of innovation and collaboration. The thermal spray community in India is not just witnessing change; it is driving it. We hope this edition sparks inspiration, fosters knowledge exchange, and fuels the passion for pushing the boundaries of thermal spray technology.

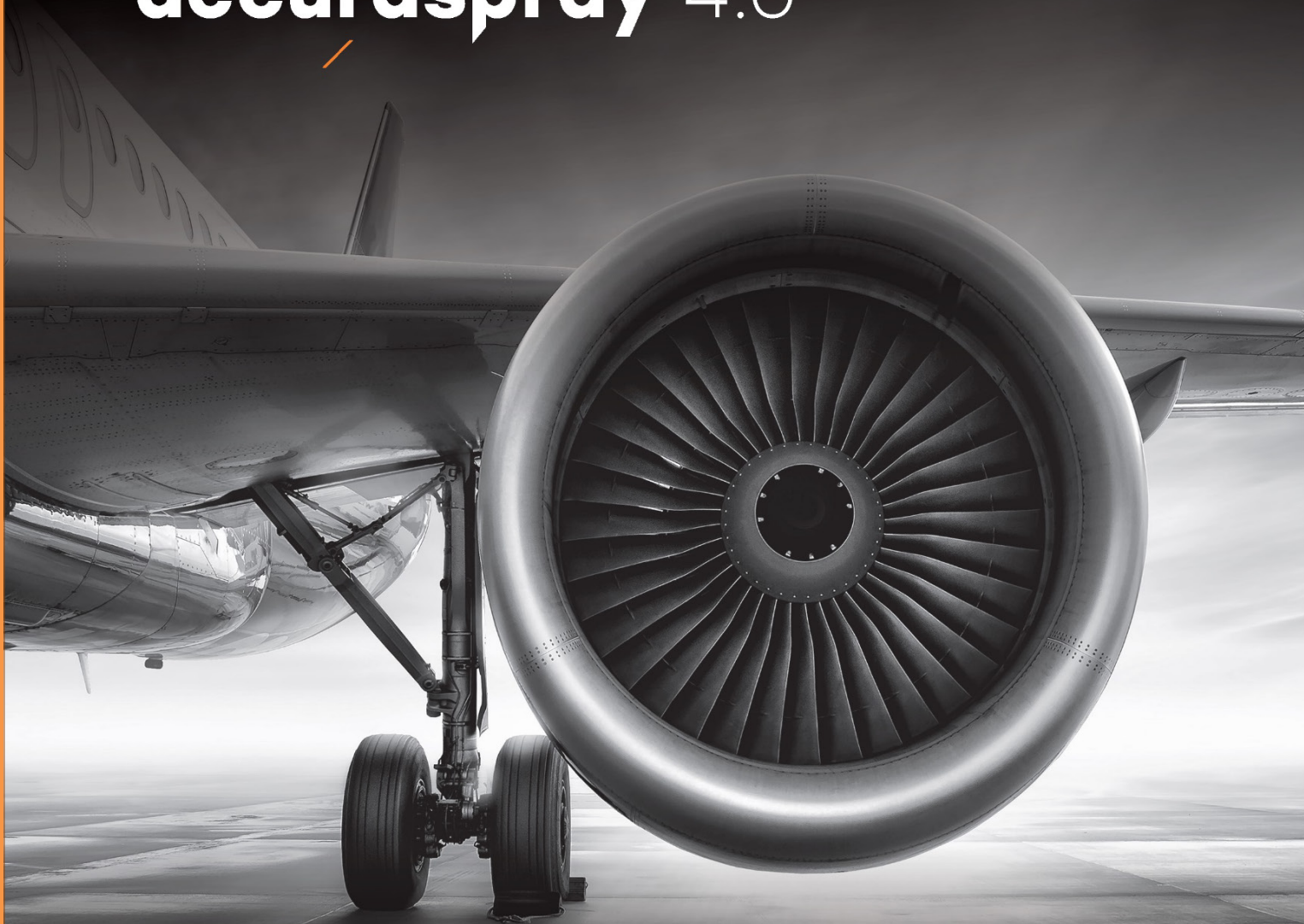
Thank you for being part of our journey. Be healthy, active, and curious!

Best Regards,

A handwritten signature in blue ink that reads "Satish". The signature is stylized and written in a cursive-like font.

(Dr. Satish Tailor)

accuraspray 4.0



Great coating every run Thermal spray sensor



The ultimate thermal spray monitoring solution
to increase productivity, streamline your processes and stay
competitive in today's research and fabrication industry.



tecnar

spraysensors.tecnar.com



NTSC-2025
National Thermal Spray Conference
& Exposition

2nd National Thermal Spray Conference & Expo

NTSC · 2025

Feb 21-23, 2025

Jointly Organized by

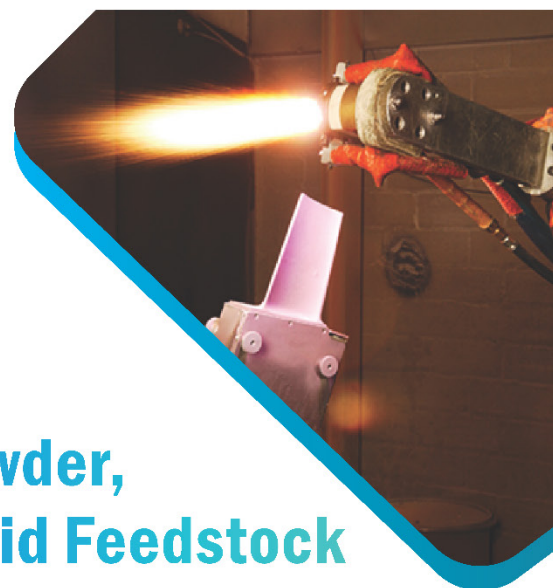
The Indian Thermal Spray Association
&

CSIR-Institute of Minerals and Materials Technology

Register today!

<https://www.indtsa.org/ntsc-2025>





Pre-Conference Course on Thermal Spraying with Fine Powder, Suspension, Solution and Hybrid Feedstock

Feb 20, 2025

Jointly Organized by
iTSA & CSIR- IMMT

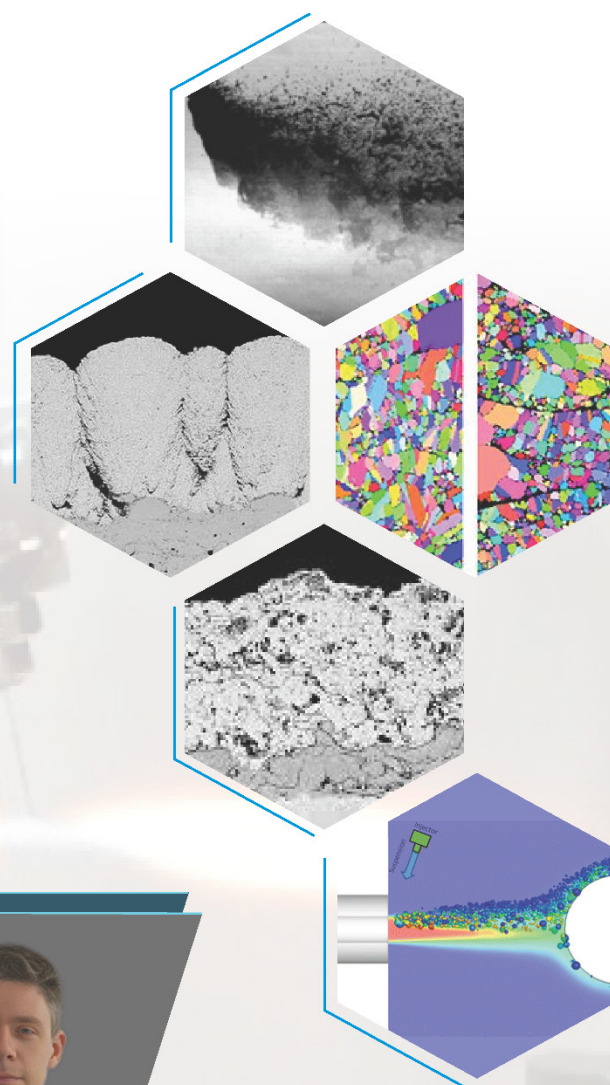
In Association with
University West & METTECH Corp.



Prof Shrikant Joshi
University West, Sweden



Dr Nicholas Curry
Consultant, Northwest METTECH Corp.



Register Now!

<https://forms.gle/hVTPdahQXk2aHFhu6>

Non-destructive Evaluation of Porosity in Thermally Sprayed Coatings Using Permeability Measurement

By **Aadil^{1,2}, Praveen R², Matt Siopsis³, Dheepa Srinivasan^{2,4}**

¹Indian Institute of Science, Bangalore -560012 (India).

²Pratt and Whitney, Research and Development Center, Bangalore – 560012 (India).

³Pratt & Whitney, East Hartford, United States.

⁴ MS Ramaiah University of Applied Sciences, Bangalore, India.

Email : Aadil1@iisc.ac.in

The assessment of porosity in thermally sprayed coatings, particularly ceramic coatings, is a challenging and error-prone task due to artifacts associated with metallographic specimen preparation. Existing methods for porosity evaluation in thermal spray coatings are predominantly qualitative in nature. This article is an attempt to enable a more quantitative measurement of the porosity using a permeability tester based on the principles of pressure drop across a porous framework, using a Kermetico permeability rig on an air plasma sprayed MCrAlN coating with an unknown porosity. Porosity and volume fraction of the coating were evaluated and validated using microscopy and a transfer function was established, correlating permeability with pore size.

Thermally sprayed coatings, such as thermal barrier coatings (TBCs), are engineered to be porous to maximize their thermal insulation performance (Ref. 1-2). The porosity ranges from 5-25%, based on the actual component and application, such as for oxidation and thermal protection or for use as an abradable coating (Ref. 3). For many of the functional applications, it becomes very challenging to get reliable and repeatable data on the coating porosity. Establishing the coating thickness, porosity, and interfacial characteristics (with the substrate) are part of the production quality control processes (Ref 4). The current process for evaluating the coating quality is via metallographic analysis which involves subjecting the coating through a rigorous mechanically intense process such as sectioning, mounting, grinding, and polishing, which can result in significant damage and cause pull outs that may exaggerate the sample porosity and may tend to

cause rejections in the coating during quality control (Ref 5, 6). It therefore becomes imperative to develop other methods of assessing the coating quality, especially via non-destructive techniques. Non-destructive techniques such as pycnometry (Ref 7), gamma-ray transmission (GRT) (Ref 8), X-ray computer tomography (CT) (Ref 9), Ultrasonic testing (Ref 10), Infrared thermography (Ref 11), and Terahertz time-domain spectroscopy (Ref 12) have been attempted, and have their respective merits and de-merits. There is a need for a simpler and agile technique to assess thermally sprayed coatings porosity during production.

In this study, a Kermetico permeability rig (Fig. 1a) was used to measure the volumetric fluid flow rate through porous coatings by using the pressure drop across the coating, placed along with sintered porous discs of known porosity. This technique, designed for calculating the volume fraction of interconnected pores, requires a free-standing coating for qualification, making it an effective candidate for non-destructive evaluation in production settings. The purpose of this effort is to establish a reliable baseline for using this permeability rig to evaluate porosity in abradable coatings by identifying the correct porous disc for spraying. Assuming negligible inertia for gas through interconnected pores, the coefficient of viscous Gas Permeability (Y_n) is calculated using Darcy's equation Eq. (1), which considers the pressure gradient (ΔP), thickness of the sample (d), cross-sectional area (A), dynamic viscosity (η), and volumetric flow rate (Q) of the test fluid.

$$Y_n = \frac{Q \cdot \eta \cdot d}{A \cdot \Delta P} \quad [1]$$

The rig comprises of a pressure gauge, pressure regulator, two flowmeters, and a test cell with specific technical characteristics as shown in Fig. 1a. The working range of the permeability rig with compressed air / nitrogen as the fluid is $(0.01-21) \times 10^5$ Pa. To start with, the pressure regulator is connected to compressed air. A 210 Soft Buna-N O-ring was placed in the chamber as shown in Fig. 1b, to ensure an airtight stack for measuring accurate fluid flow across the sample of interest, with grease applied to the O-ring to ensure a leak proof interface (Fig. 1c). The free-standing coating was placed on top of the O-ring, followed by the porous sintered disc, as shown in the schematic Fig. 1(d). The cell lid was secured with four thumb screws, and compressed air was passed through the combination of porous sintered disc (P), free standing coating (referred to as 'dummy coating - 'D') and the O-ring 'O'. The pressure was controlled by the pressure regulator and recorded by an electronic pressure gauge, as shown in Fig. 1a. The rig consisted of two flow meters (I and II) with maximum flow rates (Q) of 5.6 ml/min and 51 ml/min.

A NiCrAlW air plasma sprayed free standing abrasible coating of unknown porosity was taken as the test sample 'D', in the form of a disc having a diameter of 25.4 mm and 2.47 mm thickness. Porous stainless-steel sintered discs, with a pore size of 2, 5, 10, 20 and 40 μ m, were procured from McMaster, USA, and verified for porosity using scanning electron microscopy (Carl Zeiss, Ultra55, FESEM). Fig. 2 shows representative SEM micrographs of porous discs of 2 μ m (Fig. 2a) and 40 μ m (Fig. 2b) to indicate the pore sizes (inserts). Fig 2c is a representative SEM micrograph of the NiCrAlW coating with unknown porosity. The nominal composition of the coating was 71.92% Ni, 9.14% Cr, 7.47% Al, and 11.46% W as measured using Energy dispersive X-ray spectroscopy (EDS).

To characterize the pore size of the coating (D) with unknown porosity, combinations of the porous discs (P) and Dummy (D) were utilized in three different configurations along with the O-ring (O), designated as OD, OP, and ODP, as depicted in Fig. 3. For each configuration, nine trials were conducted by three separate operators to ensure the repeatability of the flow data.

OP showed high permeability across all pore sizes from 2 μ m, 5 μ m, 10 μ m, 20 μ m, and 40 μ m) and did not show any sensitivity to the pressure. In fact, at very low pressures, the flow maxed out indicating that each disc offered

minimal resistance to gas flow, owing to the open pore network within the sintered discs allow free flow of the gas with little or no resistance. OD on the other hand exhibited a permeability of $1.4 \times 10^{-22} m^2$. The systematic variation of permeability with ODP with different sintered discs is shown in Fig. 4, indicating a linear relationship between flow rate (Q) and pressure differential (ΔP), in accordance with Darcy's equation. ODP with a 2 μ m disc showed a lower slope (21.45) compared to the 20 μ m (22.59) vs the 40 μ m disc (22.54), as expected. Table 1 lists the measured slope, and the viscous permeability coefficient (γ_n) calculated using the slope.

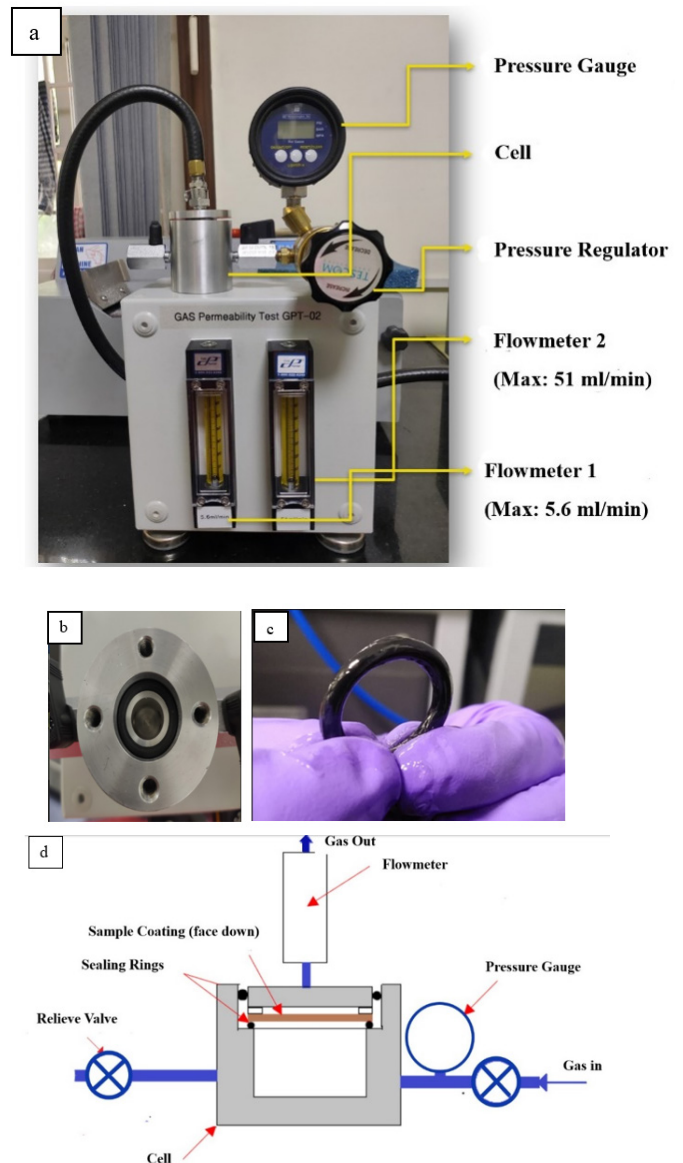


Figure 1: (a) Gas Permeability Tester (b) Experimental Cell, (c) O-ring with grease, (d) schematic of the coating gas-permeability rig

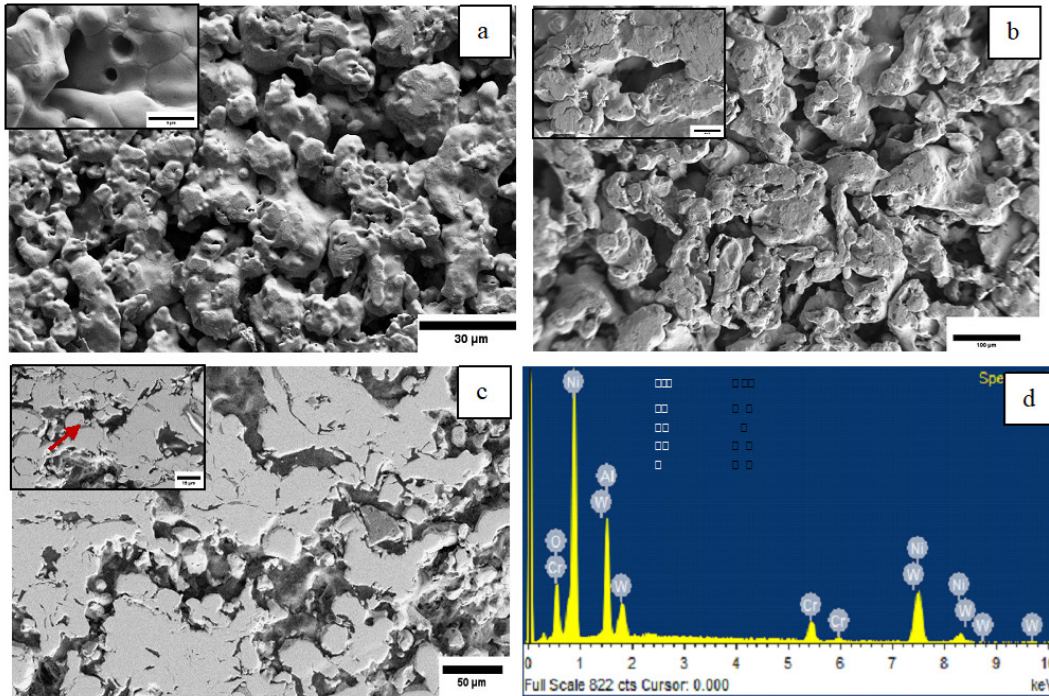


Figure 2: Representative SEM taken from (a-b) sintered porous discs with average pore sizes of 2 µm and 40 µm, (c) NiCrAlW coating along with its (d) EDS elemental spectrum

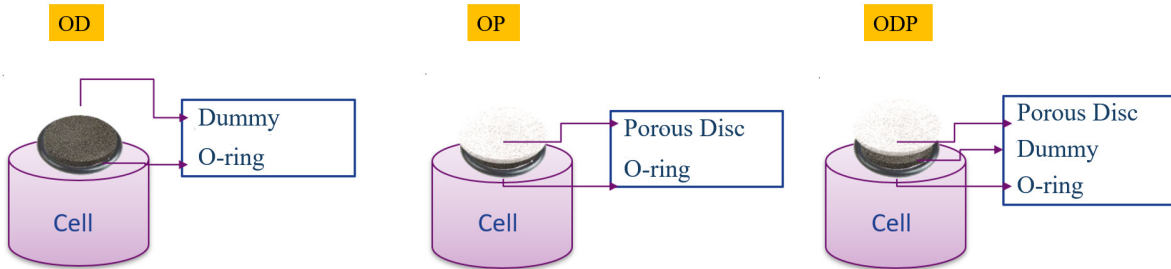


Figure 3: Configuration of, O-ring (O), 'D' and porous sintered discs (P) used for measurements

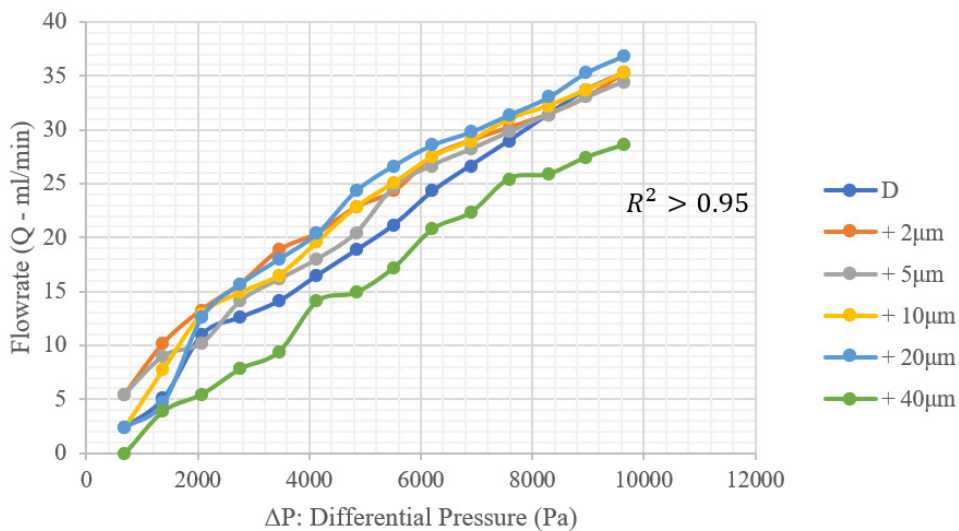


Figure 4: Flowrate Q (ml/min) vs Differential pressure

Table 1: Permeability of sample OD and ODP

Sample μm	Measured Slope	Calculated Permeability (m^2) * 10^{-22}
“D”	24.82	1.40
+ 2 μm	21.45	1.21
+ 5 μm	22.69	1.28
+ 10 μm	23.90	1.34
+ 20 μm	25.59	1.44
+ 40 μm	22.54	1.27

It is interesting to note the linear increase in permeability from $1.21 \times 10^{-22} \text{ m}^2$ (for 2 μm) with the pore size up to 20 μm ($1.44 \times 10^{-22} \text{ m}^2$) and the dip to $1.27 \times 10^{-22} \text{ m}^2$ for the 40 μm sintered disc. This clearly brings in the choice of sintered disc for carrying out the measurements on the coating with unknown porosity and brings in the interplay between the restricted flow between the coating and the pore size of the disc. For smaller pore sizes (2 μm and 5 μm), the disc introduces an additional bottleneck, limiting the flow more than discs with large pores. As pore size increases (10 μm and 20 μm), there is a larger volumetric flow diminishes, and the permeability of ODP approaches that of the coating alone ($1.4 \times 10^{-22} \text{ m}^2$). As the sintered discs pore size increases further, to 40 μm , the sheer volume of flow ceases to have any significant effect on the pressure drop and possibly the thicker framework of the disc serving to block accessibility of gas flow through the coating and hence reduce the overall permeability.

Plotting permeability versus pore size of ‘P’, gives an inverted bell curve as shown in Fig. 5. This was fit into a parabolic curve between pore size (x) and permeability (y) as represented below in Eq. 2:

$$y = -6 \times 10^{-26}x^2 + 2 \times 10^{-24}x + 1 \times 10^{-22} \quad [2]$$

By considering the ODP samples as a series of membranes comprising two flow resistances (D and P), Eqn. 2 can be used to determine the effective pore size for the coating with unknown porosity ‘D’, Interpolating the permeability of OD ($1.4 \times 10^{-22} \text{ m}^2$), into Eq. 2, The pore size associated with the ‘D’ coating was calculated to be 13.71 to 31.06 μm (as shown via dotted lines in Fig. 5). This was seen to correspond with the measurement made via the SEM image (Fig. 1c), showing a range of 15-20 μm for ‘D’.

Thus, this preliminary study is a simple demonstration of the use of a non-destructive technique for measuring porosity in plasma-sprayed coatings using the Kermetico rig. The key takes away from this is to enable the right set of porous sintered disc to choose for effective

measurement of porosity, based on volumetric flow is valid for pressure drop across interconnected porosity in thermal sprayed coatings.

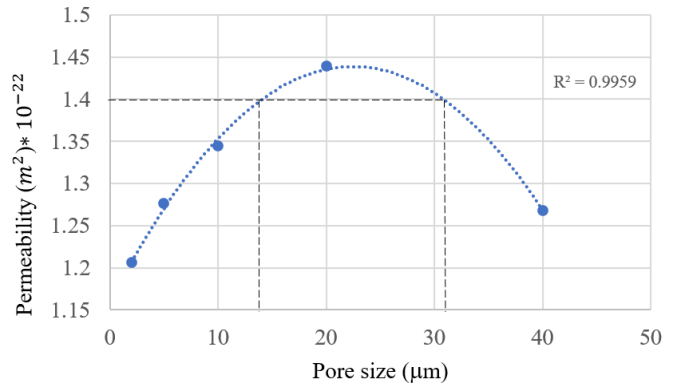


Figure 5: Permeability of the combination (ODP) vs pore size of porous disc

Acknowledgments

Mr. Andrew A. Verstak from Kermetico Inc is acknowledged for his valuable discussion. Pratt & Whitney is acknowledged for enabling the internship for Mr. Aadil, at the Pratt & Whitney R&D Center, Bangalore. The usage of characterization facilities at the Center for Nanoscience and Engineering (CeNSE), IISc, is gratefully acknowledged.

References

1. T. Shun Dong, R. Wang, Y. Lan Di, H. Dou Wang, G. Lu Li, and L. Liu, High Temperature Oxidation Resistance and Thermal Growth Oxides Formation and Growth Mechanism of Double-Layer Thermal Barrier Coatings, *J Alloys Compd*, Elsevier Ltd, 2019, 798, p 773-783, doi:10.1016/J.JALLCOM.2019.05.052.
2. N.P. Padture, M. Gell, and E.H. Jordan, Thermal Barrier Coatings for Gas-Turbine Engine Applications, *Science*, Science, 2002, 296(5566), p 280-284, doi:10.1126/SCIENCE.1068609.
3. J. Huang, X. Cao, W. Chen, X. Guo, M. Li, W. Wang, S. Dong, L. Liu, and M. Chen, A Comprehensive Review of Thermally Sprayed Abradable Sealing Coatings: Focusing on Abradability, *Chinese Journal of Aeronautics*, Elsevier, 2024, 37 (10), pp. 1-25.
4. Q. Liu, S. Huang, and A. He, Composite Ceramics Thermal Barrier Coatings of Yttria Stabilized Zirconia for Aero-Engines, *J Mater Sci Technol*, Chinese Society of Metals, 2019, 35(12), p 2814-2823.
5. R.E. Chinn, Chapter 4. Grinding and Polishing, *Ceramography: Preparation and Analysis of Ceramic Microstructures*, ASM International, 2002, 34, p 468-469, <https://www.asminternational.org/books-and-handbooks/results/>

- [/journal_content/56/10192/06958G/PUBLICATION/](#)
Accessed 10 February 2024.
6. "Metallography: Principles and Practice - ASM International," n.d., https://www.asminternational.org/books-and-handbooks/results-/journal_content/56/10192/06785G/PUBLICATION/
Accessed 10 February 2024.
 7. V. Matko, "Determination of Porosity Using a Water Pycnometer with Capacitive Level Detection," Sensors and Materials, 2004.
 8. M. V. Oliveira, A.A. Ribeiro, A.C. Moreira, A.M.C. Moraes, C.R. Appoloni, and L.C. Pereira, Comparison of Porosity Measurement Techniques for Porous Titanium Scaffolds Evaluation, Materials Science Forum, Trans Tech Publications Ltd, 2010, 660–661, p 100–105.
 9. H. Taud, R. Martinez-Angeles, J.F. Parrot, and L. Hernandez-Escobedo, Porosity Estimation Method by X-Ray Computed Tomography, J Pet Sci Eng, Elsevier, 2005, 47(3–4), p 209–217.
 10. Y. Fan, R. Ali, S.W. King, al -Porosity, P. Heterogeneity, V.A. J Jaques, A. Du Plessis, M. Zemek, J. Šalplachta, Z. Stubianová Stubianová, T. Zikmund, and J. Kaiser, Review of Porosity Uncertainty Estimation Methods in Computed Tomography Dataset, Meas Sci Technol, IOP Publishing, 2021, 32(12), p 122001, doi:10.1088/1361-6501/AC1B40.
 11. Z. Ma, W. Zhang, Z. Luo, X. Sun, Z. Li, and L. Lin, Ultrasonic Characterization of Thermal Barrier Coatings Porosity through BP Neural Network Optimizing Gaussian Process Regression Algorithm, Ultrasonics, Elsevier, 2020, 100, p 105981.
 12. M.P. Connolly, The Measurement of Porosity in Composite Materials Using Infrared Thermography, Sage Publications Sage CA: Thousand Oaks, CA, 1992, 11(12), p 1367–1375, doi:10.1177/073168449201101203.
 13. H. Wang, Q. Yang, X. Peng, F. Qin, R. Li, D. Ye, Q. Zhang, J. Xu, and J. Pan, Nondestructive Evaluation of Thermal Barrier Coatings' Porosity Based on Terahertz Multi-Feature Fusion and a Machine Learning Approach, Applied Sciences 2023, Vol. 13, Page 8988, Multidisciplinary Digital Publishing Institute, 2023, 13(15), p 8988, doi:10.3390/AP13158988.
 14. "Instant Gas Permeability Tester for a Coating Test. Measure Porosity of a Sprayed Metals Quickly,," n.d., <https://kermetico.com/control-and-auxiliary/gas-permeability-tester-thermal-spray-coatings-porosity-measurement> Accessed 10 February 2024.

Thermal Spray Training and Certification

The **Indian Thermal Spray Association** offer training and certification course on "**Thermal Spray Coating Applicator/Operator**" and "**Thermal Spray Coating Inspector**" levels following **ISO 14918, AWS C2.16/C2.16M & AWS C2.23M** standards on the following thermal spray processes-

- Thermal Spray Aluminum (TSA)
- Thermal Spray Zinc (TSZ)
- Twin Wire Arc Spray
- Wire Flame Spray
- Powder Flame Spray
- High Velocity Oxy-Fuel (HVOF)
- Plasma Spray
- Cold Spray

In order to ensure personalized attention and effective learning, each batch will accommodate limited candidates. Therefore, seats are limited, and we encourage you to secure your spot at the earliest opportunity. Don't miss this chance to elevate your expertise in thermal spray technology and stay ahead in your industry. Please contact us for more info & fee at info@indtsa.org



An Attempt to Understand Stainless 316 Powders for Cold-Spray Deposition

By **Neeraj S Karmarkar¹**, **Vikram V Varadaraajan¹**, **Pravansu S Mohanty²**
and **Sharan Kumar Nagendiran¹**

¹Dept. of Mechanical Energy University of Michigan-Dearborn

²Paul K. Trojan Collegiate Professor of Engineering, Mechanical Engineering, University of Michigan Dearborn.

Email: nkarmark@umich.edu

Abstract

Cold gas dynamic spray (CS) is a unique technique for depositing material using high-strain-rate solid-state deformation. A major challenge for this technique is its dependence on the powder's properties, and another is the lack of standards for assessing them between lots and manufacturers. The motivation of this research was to understand the variability in powder atomization techniques for stainless steel powders and their subsequent properties for their corresponding impacts on CS. A drastic difference (~30%) was observed in the deposition efficiencies (DEs) of unaltered, spherical and similar sized stainless steel (316) powders produced using centrifugal (C.A) and traditional gas atomization (G.A) techniques. The study highlights more on the differences on a precursor level.

Introduction

Cold spraying of austenitic stainless steels is widely used to improve surface corrosion resistance and is well studied by several researchers. In the CS study using water atomized (W.A), and gas atomized (G.A) stainless steel powders extensive deformation was observed in W.A powder leading to more hardness in its coating [1]. The irregular powder morphology results in better drag characteristics resulting in higher particle velocities [1]. Brewer's study [2] compares 3 different G.A stainless-steel 316 powders with different particle distribution and observes different initial phases in the powders. They recorded a variation in atomized powders between batches/lots and manufacturers. These have been systematically identified as factors that affect CS deposition. Centrifugal atomization (C.A) is a process that

utilizes centrifugal forces to break up a rotating sheet of liquid into fine droplets. While C.A powders are widely used in additive manufacturing, powder metallurgy, limited information is available on its use with CS [3, 4]. Unlike two-fluid atomization techniques, the centrifugal process can be controlled better and can achieve a narrow particle size distribution (PSD). This process also results in higher solidification rates 108 °Cs-1 with respect to G.A 106 °Cs-1 and W.A 107 °Cs-1 atomization techniques [5]. C.A technique typically produces powders with higher density, similar sphericity and roundness compared to gas atomization. Hence comparing the properties of C.A and G.A powder would improve the understanding of their impact on CS ability and assist towards the development of powder production for CS. This article emphasizes more towards powder assessment, and significant coating properties are presented.

Experimental

Stainless Steel 316 powders with identical composition mentioned in Table 1 were used for this study. These powders had an identical PSD. These powders were used to spray cold spray coatings on aluminum substrates with identical parameters. Further details regarding experimental methods are documented in the published article <https://doi.org/10.3390/powders2010011>

Table 1: Chemical composition of powders used for cold spray

Composition	Fe	Cr	Ni	Mn	C	Mo	Si	P	O	N
G.A powder	Bal	16.9	11.59	0.46	0.02	2.39	0.7	0.04	.03	.01
C.A powder	Bal	17	11.5	1.35	0.03	2.16	0.87	0.037	.04	.0588

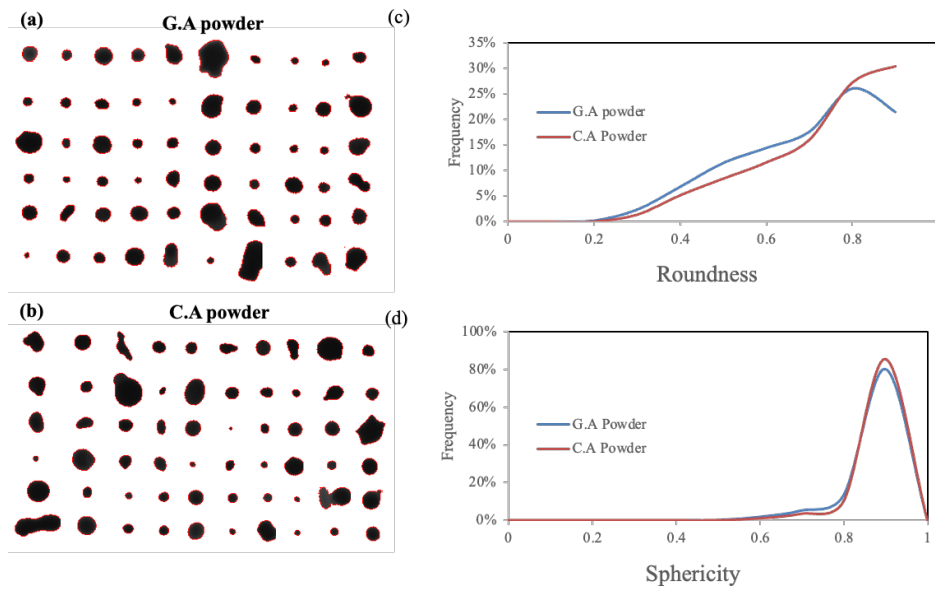


Figure 1: Snapshot of the powder particles from the shape analyzer (a,b) roundness (c) and sphericity (d) distribution of both powders

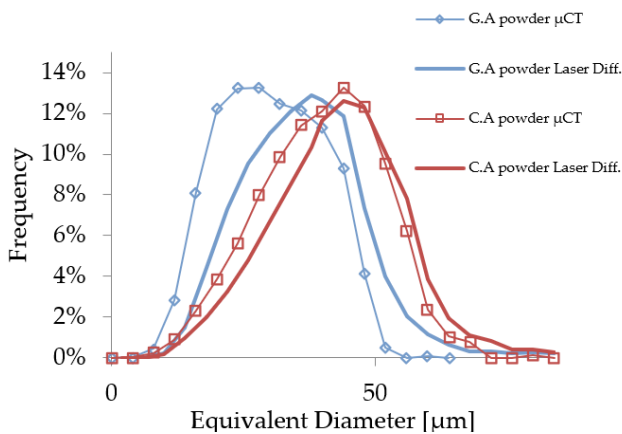


Figure 2: Particle Size Distribution for both stainless steel powders obtained using laser diffraction and μCT techniques

Discussion

Powders obtained from C.A and G.A techniques were spherical. C.A powder showed less agglomerated satellites relative to the G.A powder. These satellites may be postulated to have significant variances in the deposition efficiency of the cold sprayed coating. Particle size distribution (μCT and Laser diffraction) and 3D characterization was measured for both precursors as shown in Figure 1, 2 and 3. These results showed some minor differences between both the powders possibly due to presence of agglomerates. The C.A powders exhibited higher sphericity and roundness above a 35μm size. C.A powders had a significantly lower fraction of fine pores and larger fraction of coarse pores compared to G.A. At dimensions between 30-60μm C.A powders exhibited higher porosity.

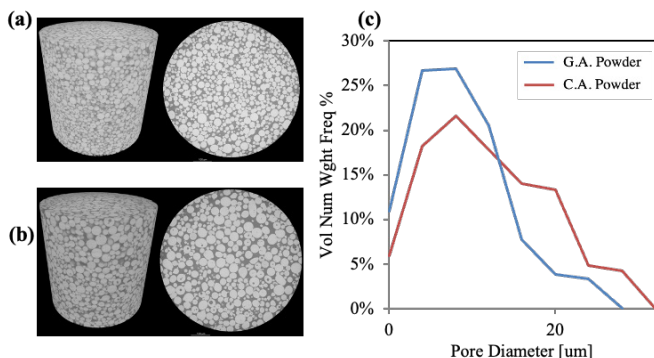


Figure 3: μCT scan results – snapshot of the scan volume (a) G.A powder (b) C.A powder (c) Pore size distribution

Powder characterization was also done using XRD and EBSD analysis. Figure 4. shows EBSD scans (IPF and Phase maps). It was clearly noticed that the ferrite content present in smaller fragments of the powder can be associated with the higher solidification rates of the particle. A significantly lower fraction of grain boundaries <5 deg was observed with C.A powder. This can be associated with the solidification rates of the C.A powder. Larger grains were present in the C.A powder as seen in Figure 5. G.A powders had a high fraction of the LAGB leading to grain coarsening. Nano hardness was measured on the cross-section surface of both powder particles. Various areas within the particle were intended to delineate the differences within the particle. The nano-

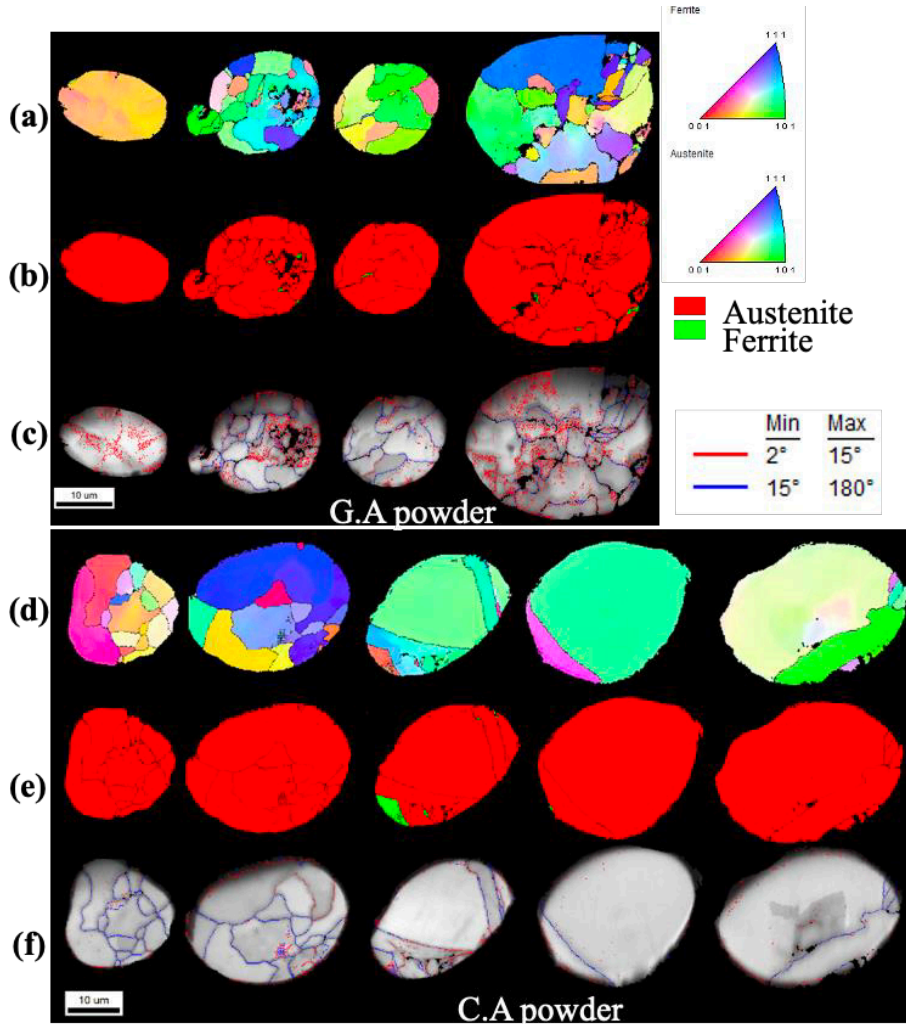


Figure 4: EBSD data IPF (a,d) Phase map (b,e) IQ map with red ($>2^\circ, <15^\circ$) LAGB and blue HAGB ($>15^\circ$) boundaries (c,f) for G.A and C.A powders respectively

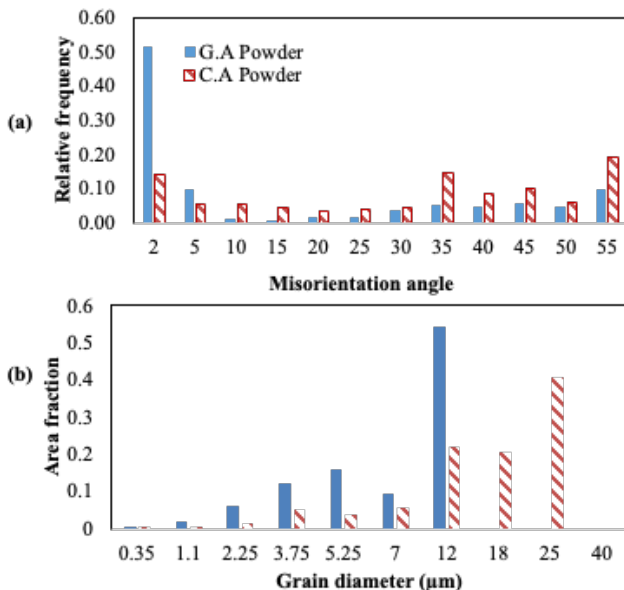


Figure 5: Total misorientation (a) and grain size distribution (b) obtained from the G.A and C.A powder EBSD scans

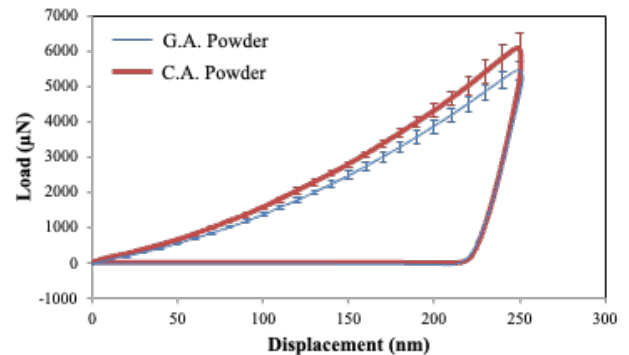


Figure 6: Force-Displacement curves for C.A and G.A powders (nano-indentation)

indentation curves are shown in Figure. 6. This curve represents an average and 3σ distribution in the loading section of the test. The C.A particles required a higher load for the given indenter displacement. An average hardness of 2.65 GPa and 2.87 GPa was recorded for G.A and C.A powders respectively. This higher hardness in the

C.A powder could be due to the higher fraction of HAGB observed with EBSD measurements. The difference in cooling rates during atomization could be another contributing factor. Other differences in hardness could be due to grain orientation with respect to nano indent and has been studied by other researchers too.

Cold sprayed coatings were sprayed on large aluminum plates to delineate the differences in deposition characteristics. While keeping the deposition parameters constant, both the coatings were sprayed to achieve ~1.3mm thickness. For this sprayed thickness a significant difference in deposition efficiency was observed between G.A and C.A powder, the latter being lower. Table 2 shows details about the deposition cycles. Both C.A and G.A coatings showed similar low microhardness (HV0.3) hardness levels near the bond line. However, with increasing the distance from the bond line only the G.A coating demonstrated a corresponding increase in hardness. The C.A coating had a monotonic hardness value of ~220 HV from the substrate to the free surface indicating lack of cold work and a low degree of deformation. Table 3 represents the results of the bond test. G.A coating showed higher bond strength than C.A coating. The location of bond failure is critical to understanding the bond quality of the coatings. The G.A coating experience adhesive failure of the FM1000 epoxy. For the C.A coating, cohesive failure occurred until at the initial layers of deposition. This shows that the bond strength for G.A coatings could be greater than 70MPa and C.A coatings failed at 45 MPa tensile strength. The lack of deformation or cold work in the C.A coating observed from the monotonic hardness levels showed a poor mechanical anchoring reducing the bond strength of the C.A coating significantly.

Table 2: Cold spray coating parameters

(a)	Temperature (°C)	Pressure (MPa/psi)	Standoff (mm)	Carrier Gas (MPa/psi)	Powder flow (g/min)
	600	3.447/500	10	0.47/68	20
(b)	Powder	Layers to achieve ~1.3mm coating thickness	Deposition time	Deposition Efficiency (%)	
	G.A	4	32mins 28sec	70.26±0.3	
	C.A	6	48mins 52sec	41.33±0.92	

Table 3: Bond strength of the coatings

	Bond strength (MPa)
G.A Coating	68.125 ± 1.10
C.A Coating	47.5 ± 0.76

Conclusions

The atomization techniques had a significant impact on the deforming mechanisms for cold spray. Despite similar morphological characteristics C.A powders had a significantly lesser DE compared to G.A powders. Analysis of the C.A coatings revealed a lack of bonding between C.A particles which was evident from its lower bond-strength. Aside from the slightly larger powder size difference (which was identified much later in the investigation), EBSD and Nanoindentation measurements revealed some distinct differences between the powders. This study found powder nano-indentation to be a reliable technique for evaluating cold-spray-ability of the material in terms of its deformability. Further evaluation of the analyzed EBSD data into tilt, twist and CSL boundaries will be reported in future studies. Further development in powder shape determination techniques using μCT could yield more insight into powder properties for cold spray. Low CS deposition efficiency C.A powders require further validation in terms of other materials, manufacturers, and production lots. A detailed microstructure evaluation of the cold-sprayed coatings would provide further supplementary information.

The results obtained can be connected to the variability of the production route of the powders. The microstructure in the C.A powders corresponds to the higher cooling/solidification rates used during manufacturing. This in-turn impacts its mechanical properties, internal porosity, HAGB etc. Having powder atomization process parameters in hand (which are proprietary to the manufacturer) could go a long way towards understanding and optimizing powders for cold spray. This study thus provides comprehensive information to the powder precursor assessment using state of the art characterization techniques. Such an assessment can help better understand the impact on their respective coated materials for techniques like cold spray. This will also help analyze the commercial feasibility of cold spray using all available production routes for powder manufacturing.

References

1. H. Fukanuma, N. Ohno, B. Sun and R. Huang, "1830 A Study of Stainless-Steel Deposits Sprayed by Cold Spray Process," in The proceedings of the JSME annual meeting, 2005.
2. L. Brewer, J. Schiel, E. Menon and D. Woo, "The Connections between Powder Variability and Coating Microstructures for Cold Spray Deposition of Aus-tenitic Stainless Steel," Surface and Coatings Technology, vol. 334, no. 6, pp. 50-60, 2018.
3. "Erwin Industries Centrifugal Atomization Technology," [Online].
4. V. Anglés, "ISAAC Centrifugal Atomization of Iron-Based Alloys," 2019.
5. G. Totten, "Handbook of Residual Stress and Deformation of Steel," ASM international, 2002.

Dense Sinkor® Coating for Sink Roll Application

By **Satish Tailor, Ankur Modi**

Metallizing Equipment Co. Pvt. Ltd., E-602-604, E.P.I.P. Boranada, Jodhpur, (India) – 342012
 Email: dgm_rnd@mecpl.com

Surface treatment for sink rolls in continuous galvanizing line is an important issue due to the unfavorable environment of the molten zinc. The corrosion behavior of the three types of different thermal spray coatings of WC-12Co, Al₂O₃-TiO₂, and dense Al₂O₃ (Sinkor® a MEC coating product) were tested in a static molten zinc condition for 30 days. WC-12Co coatings were prepared by HVOLF system (Make MECPL Jodhpur) equipped with MJP 5000 gun. Al₂O₃-TiO₂, and dense Al₂O₃ Sinkor® coatings were prepared by newly developed Hybrid-LVOF process equipped with CERAJET gun (Patented Technology). The full information about Hybrid-LVOF process is described by S. Tailor et al. [1-2]. The samples were analyzed for microstructure, phase and weight changes to understand the degradation mechanism of the coating after dipping in molten zinc. The results were checked and compared.

The corrosion mechanism of WC-Co coating showed Co-dissolution followed by carbide detachment from coating. Therefore, WC-Co coating is not suitable for molten zinc applications. The same results for both materials are reported by many researchers. Whereas, in contrast Al₂O₃-TiO₂ and dense Al₂O₃ Sinkor® coatings have shown good stability.

However, Zn accumulation was observed on the Al₂O₃-TiO₂ coating surface and Zn react with TiO₂ and form a Zn₂TiO₄, this leads to poor coating surface quality which can lead to poor surface quality of galvanized sheet. Therefore, Al₂O₃-TiO₂ coating also not suitable for sink rolls application.

Whereas, Hybrid-LVOF sprayed dense Al₂O₃ Sinkor® coating remained completely inert to molten zinc even after 30 days of exposure and maintains structural integrity. No visual defects and coating failure were observed even after 30 days test. The Sinkor® coating was stable without any defects and changes. No signatures were found to support in changing porosity,

formation of any new phase and accumulation on the coating surface and grain growth. It is reported that Hybrid-LVOF sprayed ceramic coatings have better mechanical and structural properties in comparison to plasma sprayed coatings [1-2], plasma sprayed coatings have more porosity and horizontal cracks after molten Zn test.

Further cross-sectioned SEM images of 0-, 10-, 20- and 30-days samples were also analyzed to investigate the penetration of molten Zn in the coatings. Microstructural analysis shows that no cracks were observed and no change in thickness was observed even after 30 days of molten zinc testing of dense Al₂O₃ Sinkor® coating. The coating remains non-reactive, and Zn shows stability in corrosive environments. Due to dense coating microstructure no zinc penetration is observed in the coatings as shown in Fig. 1. Thus, it can be said that dense Al₂O₃ Sinkor® coating does not undergo any thickness reduction and does not lose coating integrity even after 30 days of test. Moreover, no phase changes were observed. Further no stress has been generated in the Sinkor® coating.

Before weighing, samples were cleaned in an acid solution to remove any solidified zinc followed by rinsing with water and hot air drying to avoid any false indications of weight gain. The WC-12Co coating showed a decrease in weight as the dipping time increased due to Co dissolution but it was observed that the weight loss percentage is less in comparison to traditional HVOLF sprayed coating.

Whereas, Al₂O₃-TiO₂ coating showed a very marginal weight gain with the increase in dipping time due to formation of Zn₂TiO₄ on the coating surface. Sinkor® coating has shown no change in weight which shows the chemical inertness of the Sinkor® coating. The weight change data is shown graphically in Fig. 2.

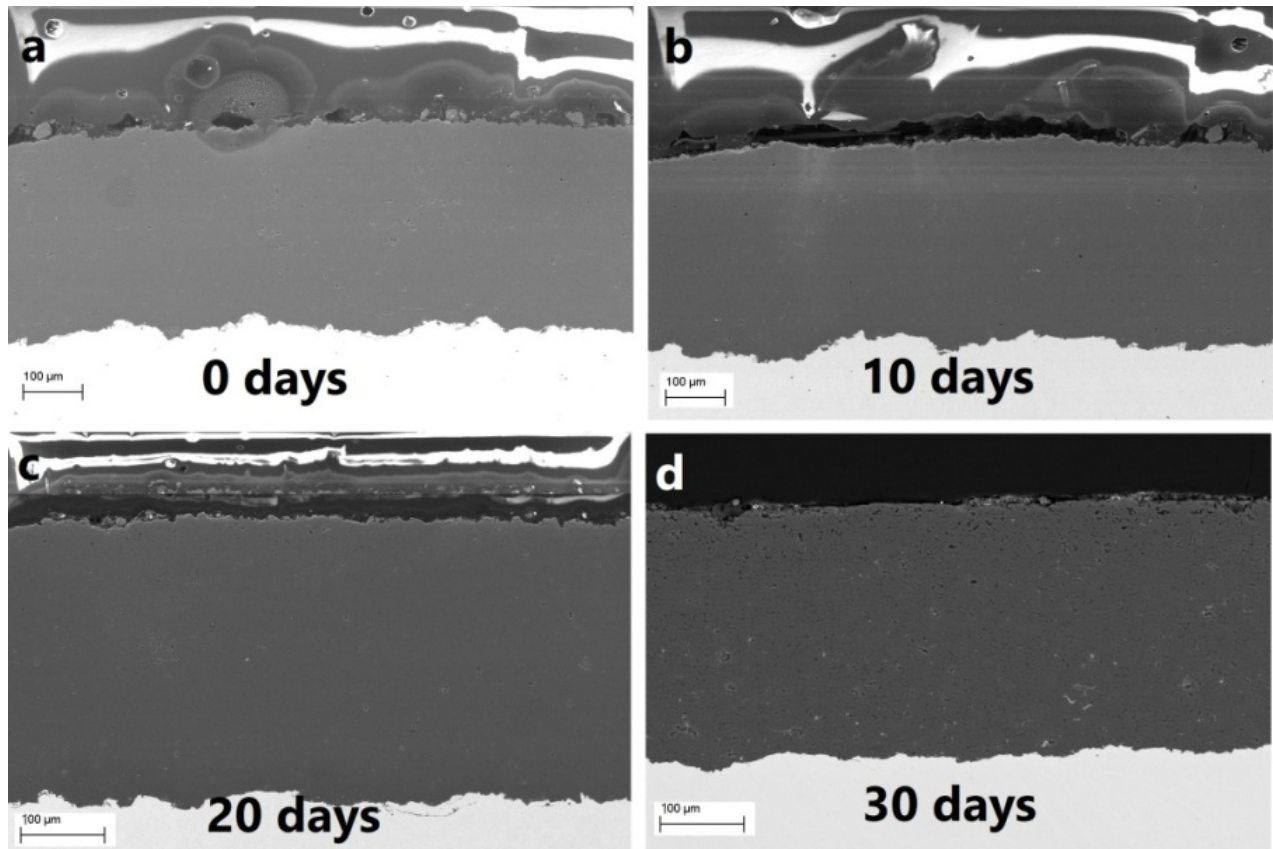


Figure 1: Sinkor® SEM microstructures after the molten zinc corrosion test for (a) 0, (b) 10, (c) 20 and (d) 30 days

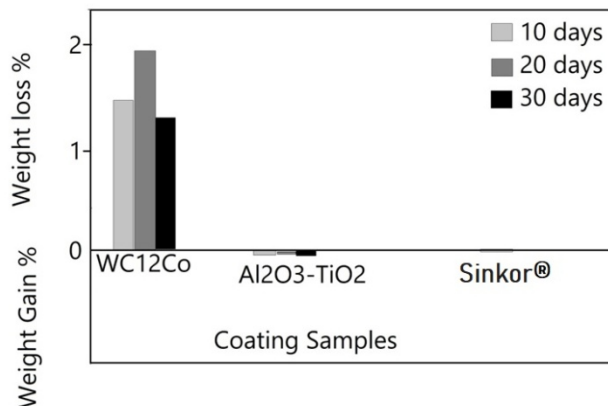


Figure 2: Weight change in coating after molten zinc corrosion test

Conclusions

The findings of this study may solve an existing major corrosion and wear problem of the steel industry associated with pot rolls, including a sink roll and two stabilizer rolls, during Galvanizing process. MECPL Jodhpur has developed a special process and coating Sinkor® to solve this problem and it could greatly improve the service life of a sink roll.

Hybrid-LVOF process is a new patented technology, mainly designed for thin and dense ceramic coatings. Hybrid-LVOF sprayed dense Sinkor® coating could be a very good solution for protecting galvanizing pot plant hardware for a prolonged duration.

References

1. Tailor, S., Vashishtha, N., Modi, A., S C Modi, High-Performance Al₂O₃ Coating by Hybrid-LVOF (Low-Velocity Oxyfuel) Process. J Therm Spray Tech 29, 1134-1143 (2020).
2. Tailor, S., Vashishtha, N., Modi, A., Modi, S.C., Microstructure evolution and mechanical properties of Al₂O₃-40%TiO₂ coating by Hybrid-Low Velocity OxyFuel process, 2021 Phys. Scr. 96 025702

For More Information, please visit published paper "Dense Al₂O₃ Coating Performance and Its Corrosion Properties in Molten Zinc for Sink Roll Applications,"

<https://doi.org/10.1016/j.ceramint.2024.11.478>

We invite you to join iTSA!



Why become a member of iTSA?

The iTSA provides useful information to all colleagues interested in thermal spraying in the large industries, societies, job shops, university and laboratories. The iTSA members have access to the additional services such as job proposition, information about services related to thermal spraying in different states of India,

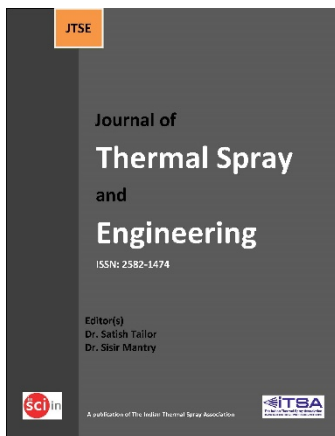
forum of users which enables research of missing information related to thermal spraying and much more. The iTSA membership also enables a reduction in the fees of the events organized by the Society.

Become a member today! <https://www.indtsa.org/join-itsa>

For more information, please visit <https://www.indtsa.org/> or write us info@indtsa.org

Our Journal Publication

Journal of Thermal Spray and Engineering (JTSE) ISSN: 2582-1474



JTSE is an international archival journal publishing scientific papers on thermal spray technology; Journal provides a platform for researchers to share their original and innovative findings, in addition to identifying methods of production and application that include, but are not limited to, HOVF, plasma spray, flame spray, wire arc spray, and cold spray, Powder technology, Gas flow, particle motion, and heat transfer, Stress and strain analysis, Coating deposition mechanism, Single particle deposition and solidification upon impact, Coating mechanical and thermal properties, Coating microstructures and phase transformation, Functional coatings, Torch design and optimization, New thermal spray technology, Robotic programming

and kinematic analysis, Torch trajectory definition and optimization, Novel applications of thermal spray coating, Mathematical and theoretical analysis on related subjects, Finite Element Analysis on related subjects. JTSE Covers Review Articles, Research Articles, Letter To Editor, Conference & Book Review, Notes and Short Communications. All the published articles are available for Download for Free.

DOI: <https://doi.org/10.52687/2582-1474/>

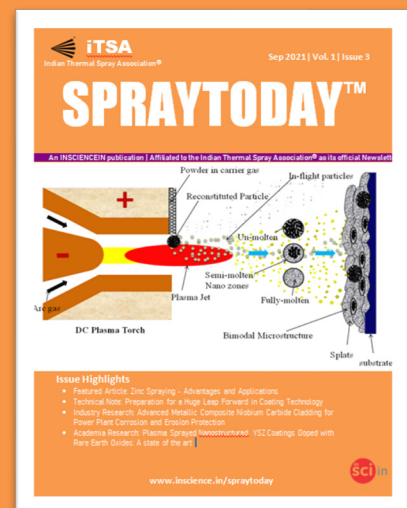
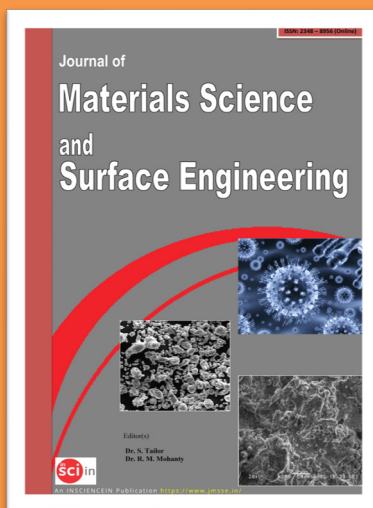
Journal website <http://www.inscience.in/JTSE.html>

Manuscript Submission <https://emmanager.in/jtse>

India's 1st thermal spray magazine...



<https://www.indtsa.org/>



<http://www.inscience.in/>

